Available online at www.sciencedirect.com
SCIENCE DIRECT
Applied Catalysis A: General 291 (2005) 162–169
APPLIED CATALYSIS A: GENERAL
www.elsevier.com/locate/apcata

Preparation of nano-gold in zeolites for CO oxidation: Effects of structures and number of ion exchange sites of zeolites

Jen-Ho Chen, Jiunn-Nan Lin, Yih-Ming Kang, Wen-Yueh Yu, Chien-Nan Kuo, Ben-Zu Wan *

Department of Chemical Engineering, National Taiwan University, Taipei 106, Taiwan

Received 28 September 2004; received in revised form 18 February 2005; accepted 18 February 2005
Available online 10 May 2005

Abstract

Nano-gold was prepared in different types of zeolite (Y, β and mordenite) in pH-adjusted chloroauric acid solution. The effects of the pore structures and the aluminum content on the loading of gold and on the reaction activity for CO oxidation at 0 °C were investigated. The gold loading in each zeolite was strongly related to the aluminum content; it was also affected by the structure of the zeolite. HRTEM results revealed that a few particles of gold around 1 nm in diameter were formed in the cage of Y-type zeolite with less aluminum loading (1.8 wt.%), and there was aggregation of gold species on the exterior surface of the zeolite; in contrast, more particles of gold around 1 nm were formed in Y-type zeolite with more aluminum loading (12.4 wt.%), no aggregation was observed. The results from the temperature-programmed reduction in hydrogen indicated that the gold species were reduced in the smaller pores (in β and mordenite) only at lower temperatures. Nevertheless, gold was easily sintered in the channels of β and mordenite during CO oxidation, causing severely reducing the activity. The cage-like pore in Y-type zeolite with 12.4 wt.% aluminum loading prevented the sintering of gold, and its hydrophilic surface favored the activation of gold species; therefore, this Au/Y catalyst exhibited high catalytic activity and stability for CO oxidation.

Keywords: Gold; Nano-gold; Zeolites; Y-type zeolite; Mordenite; β-type zeolite; CO oxidation

1. Introduction

Unlike inert bulk gold, supported gold nano-particles have been found to be very active in several reactions. Their catalytic activities depend on the support, the method of preparation, and particularly the size of the Au clusters [1,2]. Zeolite has been used as a support for loading nano-particulate gold. Gold-containing zeolites have been prepared by different methods, for the reactions of NO reduction and CO oxidation [3–12]. Au/Y (gold supported on Y-type zeolite) prepared using a chloroauric acid solution is active for CO oxidation [6–8,11,12]. Y-type zeolite has three kinds of spaces within the crystal structure [13]: the supercage with a pore opening of 7.4 Å (1 nm = 10 Å) and an inner space-diameter of 12 Å, the sodalite cage (or β-cage) with a pore opening of 2.6 Å and an inner diameter of 6.6 Å, and the hexagonal prism with a smaller opening than that of sodalite cage. In our previous work [6–8,12], temperature-programmed reduction (TPR) was employed to identify where gold species was present in Y-type zeolite. The presence of gold within the supercage and the sodalite cage indicate the small particles (less than 7.4 Å) of gold species in the solution. For instance [12], when a dilute gold solution (i.e., 0.59×10^{-3} M of gold) at pH 5 was used to prepare Au/Y, most loaded gold ions were located inside the sodalite cage of the Y-type zeolite; therefore, the major sizes of the gold species for the deposition or for the ion-exchange in this solution should be less than 2.6 Å, which is the pore opening of the sodalite cage.

Also our early work [11,14] established that gold on the surface-acidity-modified proton Y-type zeolite (by sodium ion) showed high catalytic activities and maintained good stability for removing CO at low temperature. Protons on the

* Corresponding author. Tel.: +886 2 33663021; fax: +886 2 23623040.
E-mail address: benzuwan@ntu.edu.tw (B.-Z. Wan).

0926-860X/$ – see front matter © 2005 Elsevier B.V. All rights reserved.
doi:10.1016/j.apcata.2005.02.038

zeolite catalyze the growth of larger gold particles on the surface during the process of gold loading. Moreover, the effects of the preparation conditions (for gold solution) on the activity of Au/Y were examined and well understood [12]. Accordingly, a recommended gold precursor (with sizes larger than 2.6 Å) for the preparation of Au/Y can be from a gold solution with an initial chloroauric acid concentration around 1.46×10^{-3} M and a solution pH at 6 (adjusted with NaOH solution). Au/Y with high catalytic activity can be obtained by mixing the surface-acidity-modified Y-type zeolite with as-prepared gold solution (1 g of zeolite per 125 ml solution) at 80 °C for 1–24 h.

In this study, the methods reported in our early work were used to prepare the recommended gold solution and the surface-acidity-modified supports [11,12]. Nano-gold was prepared on three different zeolites (Y, β, and mordenite) [13]. β-type zeolite contains two kinds of pores—straight and tortuous channels. The former have openings of 5.7×7.5 Å and the latter have 5.6×6.5 Å. Mordenite also contains parallel-channel pores with dimensions of 6.7×7.0 Å. Therefore, the effects of the pore openings and pore shapes of zeolite on the activity of supported nano-gold were examined. Moreover, nano-gold was prepared on Y-type zeolites with different aluminum loadings. The aluminum site in the silica framework of zeolite is the site for cation exchange. Therefore, the effect of aluminum loading in Y-type zeolite on the activity of supported nano-gold was also examined herein.

2. Experimental

2.1. Catalyst preparation

Zeolites were purchased from Conteka. Two Y-type zeolites with different aluminum loading (Y_1 and Y_2) and β zeolite were in proton forms. Mordenite was in sodium form. All the zeolites were calcined at 550 °C for 4 h and then underwent the process to modify the surface-acidity. For Y and β, the cooled zeolite was put into a 1 N $NaNO_3$ solution and the solution pH was adjusted to 6 by adding 1N NaOH solution. For mordenite, the solution pH was adjusted to 6 by adding 1N HNO_3 solution. Each sample was filtered and dried at 60 °C. The gold catalysts were prepared as follows [12]: a 250 ml volume of chloroauric acid solution of 1.46×10^{-3} M was prepared, and its pH was adjusted to 6.0 by adding NaOH solution; after 2 g of zeolite was added, the solution was heated to 80 °C and maintained at this temperature for 16 h. The supported gold samples were obtained after filtration and washing, and then dried at 60 °C. The catalysts were designated as Au/Y_1, Au/Y_2, Au/mordenite, and Au/β.

2.2. Catalyst characterization

The elemental content in each sample was determined using a GBC 906 atomic absorption unit. The reduction temperatures of the gold ions on each zeolite were obtained in a H_2/N_2 (1/9) stream, using a temperature-programmed reduction (TPR) apparatus [11,12,15]. The surface areas were measured using an ASAP 2010 Surface-Area-Pore-Volume Analyzer. XRD was carried out with a MAC Science Diffractometer (model MXP-3). HRTEM pictures were taken with a Philips CM200 transmission electron microscope operated at 200 kV with a modified specimen stage. Also, TEM pictures were taken with a Hitachi H7100 electron microscope operated at 75 kV.

2.3. Catalytic activities

Carbon monoxide was oxidized in a quartz tube reactor at 0 °C at atmospheric pressure. Catalysts that contained 0.0018 g gold and had not undergone any pretreatment in the reactor were used for CO oxidation. During the reaction, 32.7 ml/min of synthetic air and 0.33 ml/min of carbon monoxide were purified by molecular sieve A and mixed before the inlet of the reactor. A Shimadzu GC-8A gas chromatograph with a Carboxen™-1000 column was used to separate carbon dioxide, carbon monoxide, nitrogen and oxygen.

3. Results and discussion

3.1. Metal loading

Table 1 lists the metal loadings, the percentage of gold in the solution loaded, and the molar ratios of loaded gold to aluminum in each zeolite. The zeolite crystallinity after the loading of gold did not differ significantly from that before. Table 1 reveals that both Au/Y_1 and Au/mordenite had higher loadings of gold and aluminum than Au/Y_2 and Au/β.

Table 1
Surface area, metal loadings, gold to aluminum molar ratio, and percentage of gold in the solution loaded in each Au/zeolite catalysts

Catalysts	Surface area (m^2/g)	Metal loading (wt.%)			Molar ratio, Au/Al	Au loading percentage (%), [(Au loaded)/(Au used)] × 100
		Au	Al	Na		
Au/Y_1[a]	660	1.70	12.4	6.2	0.019	47
Au/mordenite	500	1.79	6.7	5.3	0.037	50
Au/β	650	0.88	3.2	1.8	0.038	24
Au/Y_2[a]	710	0.26	1.8	0.7	0.020	7

[a] Y_1 and Y_2 are Y type zeolite.

Therefore, almost 50% of the gold in the gold colloid solution was loaded on Y_1 and mordenite during the preparation. Nevertheless, less than 25 and 10% of the gold in the solution were on β and Y_2 zeolites. Notably, the amount of loaded gold was strongly correlated with the amount of aluminum in each zeolite. Accordingly, the molar ratios of gold to aluminum in Table 1 indicates that for a given cage structure of zeolite (Y_1 and Y_2), the ratios were approximately the same; for the zeolite with the channeled structures (mordenite and β), even though the sizes and shapes of the channels were not exactly the same, the ratios were in a close range. Nevertheless, the molar ratios of gold to aluminum in the channel-type zeolite exceeded those in the cage-type. The higher ratios follow from the fact that all of the aluminum in the channels of mordenite and β can be exposed to interact with gold ions in the solution during the gold loading process. However, most of aluminum in the Y-type zeolite that interacts with gold ions was from the supercage, and most aluminum in the sodalite cage was unavailable for loading gold, because the pore opening of sodalite cage was small (2.6 Å). Therefore, the results in Table 1 strongly suggest that aluminum in zeolite plays an important role for loading gold from the solution to the surface of each sample. The pore structure also substantially influences the gold loading in zeolite.

3.2. TPR profiles and TEM of Au/Y

The interactions between the gold species and the supports' surface may vary among the types of zeolite, because different zeolites have different structures and may have different sites for ion exchange. TPR profiles can provide such information. Fig. 1 presents the TPR spectra of fresh-dried Au/zeolites in a hydrogen-containing (H_2/N_2 = 1/9) stream. Both Au/Y_1 and Au/Y_2 show similar main reduction peaks near 106 °C. A shoulder from Au/Y_1 near 120 °C can be observed. In our earlier work [6,11,12], the primary reduction peaks represented the reduction of

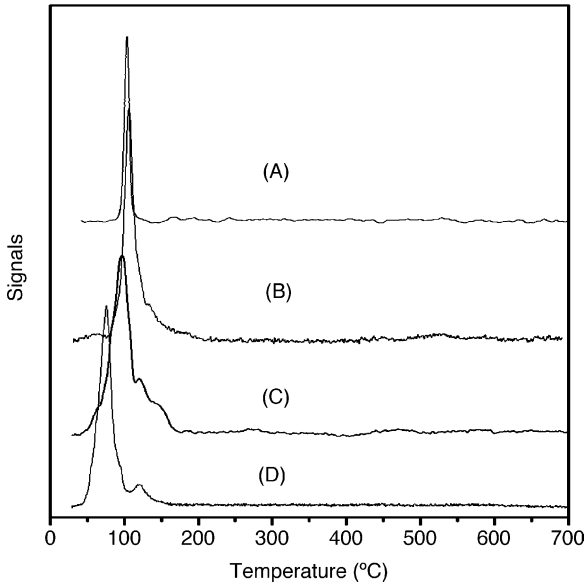

Fig. 1. TPR results of (A) Au/Y_2, (B) Au/Y_1, (C) Au/β, and (D) Au/mordenite.

gold ions in the supercages, and the shoulder represented that of the gold species on the exterior surface of zeolite particles. That the main reduction peaks are in the same positions reveals that gold species in the cages of Y_1 and Y_2 are at similar sites, although the amounts of gold and aluminum in these two supports differ considerably. The lack of an apparent shoulder from Au/Y_2 may follow simply from the fact that the amount of gold on the exterior surface of Y_2 is too small to be detected. Additionally, the HRTEM images, shown in Figs. 2 and 3, verify that small nano-gold particles with sizes around 1 nm (10 Å) in fresh-dried Au/Y_1 and Au/Y_2 were present. They were smaller than the supercage (12 Å) of Y-type zeolite, suggesting the existence of gold particles in the supercage. Only a few gold particles from Au/Y_2 were imaged by HRTEM, because a little gold was loaded on Y_2. Nevertheless, gold particles with sizes of

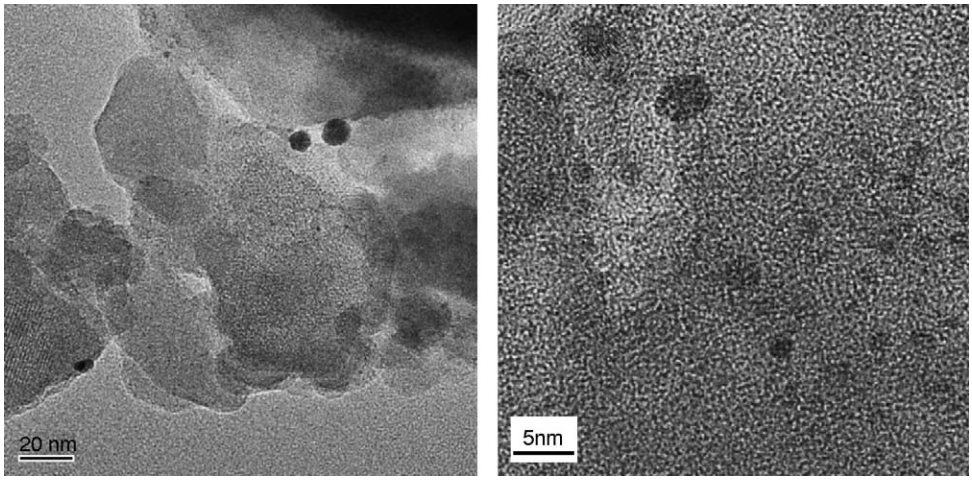

Fig. 2. HRTEM results of as-prepared Au/Y_1.

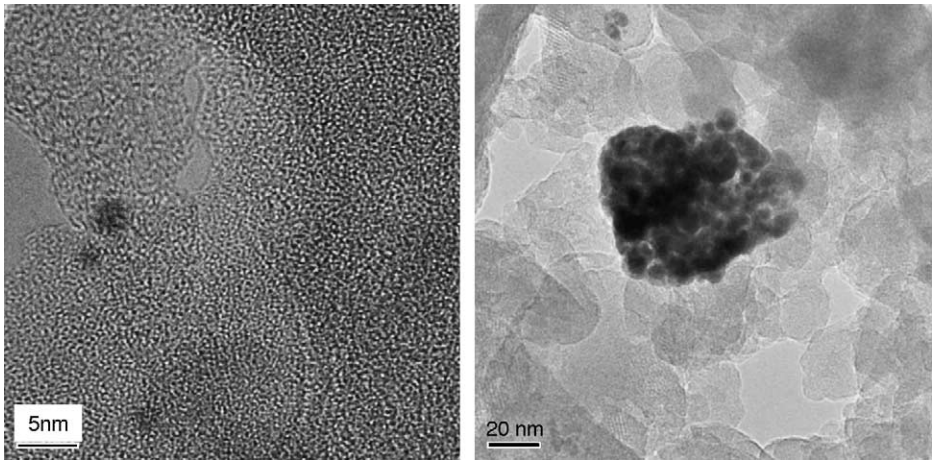

Fig. 3. HRTEM results of as-prepared Au/Y_2.

approximately 1 nm in Au/Y_2 were slightly larger than most of the gold particles in Au/Y_1. This indicates that the gold particles tend to grow larger in the supercage of Y-type zeolite with less aluminum. The growing of large gold particles was also observed on the surface of pure SiO_2 [16]. Furthermore, Fig. 3 presents gold particles that were larger than the size of supercage; in particular, there were apparent aggregation of the particles on the surface of Y_2. These particles were located on the exterior surface of Y-type zeolite. Due to no constraint from the cage, the sintering of gold on the exterior surface to the larger particles by the energy of electron beam from HRTEM is reasonable. The aggregation of large gold particles on Y_2 and the absence of such on Y_1 reveals that, the aluminum sites on the surface of zeolite can reduce the mobility of gold for sintering; therefore, the fact that the aluminum sites on Y_2 are many fewer than those on Y_1 caused the severe aggregation of large gold particles on the exterior of Y_2.

The driving force for growing large gold particles on the surface may arise from the hydroxyl group on the surface of nano-gold particles. Kung and co-workers [17–19] have presented that the gold that were active for catalytic reactions are those nano-sized gold particles, with hydroxyl group on their surface. Therefore, the reduction of gold precursors with hydrogen in the presence of water vapor is one way to activate the catalytic activity of nano-gold precursor on the support. Moreover, the presence of dilute water vapor in the nano-gold system can enhance catalytic activity [14,20–23]. However, in this study the hydroxyl group on the surface of the gold precursor or the nano-gold metal is believed to be able to cause the sintering on the support surface, because the hydrogen bond on the hydroxyl group can raise strong hydrophilic interaction among gold particles. The subsequent condensation of water from the hydroxyl groups between the particles causes the sintering of gold. On the other hand, the interaction between the hydroxyl group on gold and the ion exchange sites on zeolite can reduce the mobility of gold particles on zeolite surface for sintering. Therefore, the TEM pictures in Fig. 4 reveal that the sizes of most gold particles on Au/Y_1 were smaller than those on Au/Y_2, after the samples were reduced at 600 °C under 30 ml/min flow of H_2/N_2 (1/9) for 2 h. The fact that the number of ion-exchange sites on Y_1 greatly exceeded the number on Y_2 was the main reason for the less sintering of gold on Y_1, even though the density of gold particles (particles per surface area) on the surface of Au/Y_1 (which factor also influence sintering) was much higher than that on Au/Y_2.

3.3. TEM and TPR profiles of Au/mordenite and Au/β

Fig. 4 reveals that the sizes of the gold particle on Au/β were similar to those on Au/Y_2, and were slightly larger than those on Au/mordenite, after the samples were reduced at 600 °C, a high temperature. These are because the aluminum loading in generating the ion exchange sites on the surface of Au/β was close to that of Au/Y_2, and was much less than that of Au/mordenite. Interestingly, although the gold loading in Au/mordenite was higher than that in Au/Y_1, the number of gold particles on Au/mordenite in the TEM pictures was substantially less than the number on Au/Y_1. This is perhaps because of the severe sintering of gold on Au/mordenite and Au/β following the treatment at high temperature; therefore, the twisted bars or chunks are observed in TEM pictures of both samples. Nevertheless, the bars or chunks were not observed from Au/Y samples. These gold bars or chunks were believed to arise from the sintering of gold in the channels of Au/β and Au/mordenite during the rise in temperature and under high-temperature reduction conditions. They migrated out of the channels to form larger bars and chunks observed in TEM pictures. In contrast, the presence of cage-like pores in Y-type zeolite prevents the formation of gold bars in the pores from Au/Y samples.

The TPR spectra of fresh-dried Au/mordenite and Au/β, presented in Fig. 1, differ from each other and from those of Y-type zeolites. These strongly demonstrate that the sites of different types of zeolite for loading gold in the solution indeed differ. The main reduction occurred at 74 °C and an apparent shoulder was observed at 120 °C from

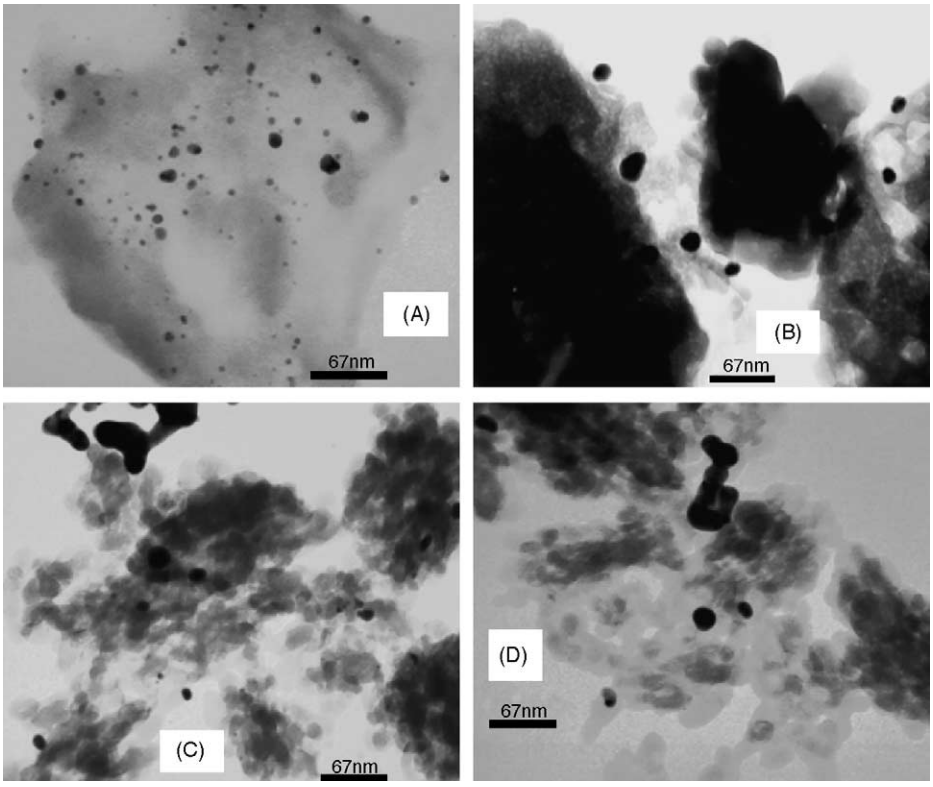

Fig. 4. TEM results of gold catalysts after high temperature reduction under H_2/N_2 (1/9) flow at 600 °C for 2 h, (A) Au/Y_1, (B) Au/Y_2, (C) Au/mordenite, and (D) Au/β.

Au/mordenite. The main reduction peak from Au/β was at 94 °C and two more shoulders at approximately 120 and 150 °C appeared after the main peak.

Both Au/mordenite and Au/β showed lower main reduction temperatures than Au/Y, suggesting that the gold species were reduced more easily in Au/mordenite and Au/β than that in Au/Y. The sizes of these species in mordenite and in β were probably smaller than those in Y; therefore, these species can be reduced at the lower temperatures. The fact is reasonable, because the pore diameters (approximately 7 Å) of mordenite and β are smaller than that (12 Å) of the supercage in Y-type zeolite. Apparently, gold species grew on the support surface during the gold loading process, causing larger gold species to be formed in the larger pores. Additionally, Fig. 1 reveals that the main reduction peak from Au/β was broader and slightly higher than that from Au/mordenite. The broader peak can be de-convoluted into two, and the one with the lower reduction temperature may be close to that from Au/mordenite. These findings reflect the fact that two types of channels of slightly different sizes are present in β type zeolite. Gold species in different channels were reduced at slightly different temperatures.

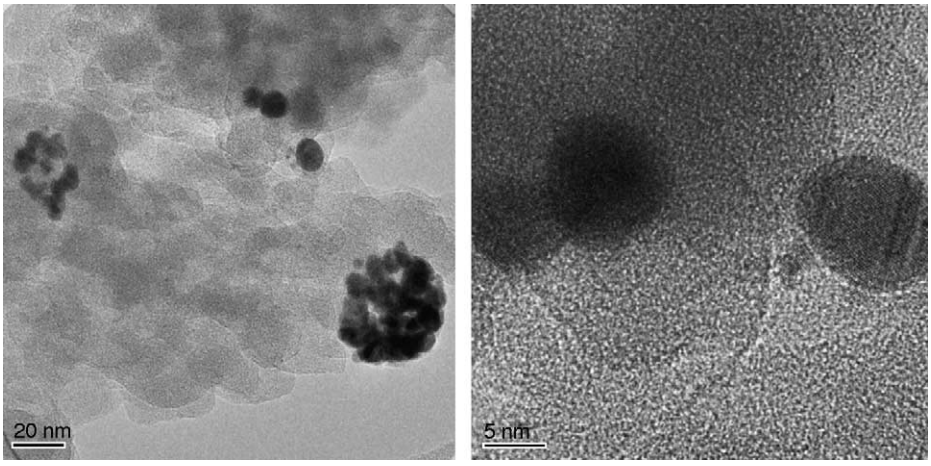

Fig. 5. HRTEM results of as-prepared Au/β.

Both Au/mordenite and Au/β exhibited reduction shoulders at 120 °C in Fig. 1. These were similar to that from Au/Y and represent the reduction of similar large gold species on the exterior surfaces of the supports. However, one more shoulder at a higher reduction temperature (150 °C) was obtained from Au/β, suggesting that larger pieces of gold were present on the exterior surface of Au/β, because two types of channels with different crystal structures were present in β-type zeolite. The exterior surfaces of these crystal structures may provide different sites for growing gold species. Therefore, without the constraint of the cage or the pore wall, differently sized gold species may grow on the exterior surface.

HRTEM resources were limited so only pictures of fresh-dried Au/β, rather than Au/mordenite, were obtained. Fig. 5 presents typical images. Since both Au/β and Au/mordenite possess similar channel-type pores and of similar pore sizes, so the results from Au/β may elucidate some of the phenomena that occur in Au/mordenite. Nevertheless, HRTEM observations in Fig. 5 reveal that no gold particles were as small as 1 nm. This result seems to contradict the results of TPR in Fig. 1, which suggested that the gold particles in Au/β and Au/mordenite should be smaller than those in Au/Y. However, gold particles of approximately 1 nm were observed in the Au/Y samples in the HRTEM pictures, shown in Figs. 2 and 3. The high energy of the electron beam during HRTEM measurement is believed to have caused the migration of gold particles out of the channels of β-type zeolite, before they were sintered into larger particles. Therefore, Fig. 5 presents gold particles larger than 1 nm, and aggregated gold particles on the exterior surface of Au/β, similar to those on Au/Y_2. The window of the cage in Y-type zeolite is smaller than the inner cage, so the particles (1 nm) that are larger than the window size do not easily migrate out of the cage. This fact may explain why the gold particles of the sizes approximately 1 nm in Au/Y samples.

3.4. CO conversions over fresh-dried gold catalysts

The activities of fresh-dried gold catalysts for CO oxidation are shown in Fig. 6. The reactions were conducted at 0 °C and only 0.0018 g of gold in each catalyst was used for the test. It can be found that it took 4 h for Au/Y_1 from an initial activity to reach a steady activity for 100% CO conversion. The lower initial catalytic activity of Au/Y_1 indicates that the gold species in fresh-dried samples were not the active sites for CO oxidation. In our previous research [11], XPS measurement revealed that the gold species in Au/Y after the tests of CO oxidation (after the initiation period) were metallic gold. The TPR experimental results (in Fig. 1) showed the ionic form of most gold species in fresh-dried Au/Y_1, suggesting that it took 4 h to reduce the majority of ionic species to the gold metal during the reaction at 0 °C. These findings indicate that the metallic gold in Au/Y_1 after initiation should be the active species for

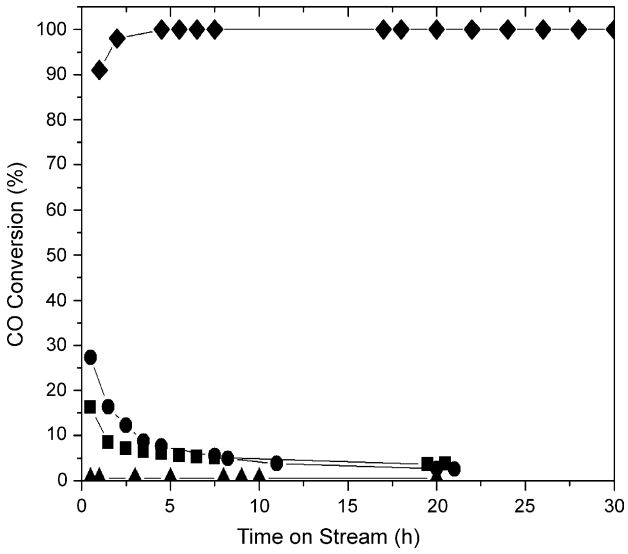

Fig. 6. CO conversion vs. time on stream at 0 °C and 1 atm total pressure over Au/Y_1 (◆), Au/β (●), Au/mordenite (■), and Au/Y_2 (▲). Each catalyst contained 0.0018 g gold. At room temperature, the total volumetric flow rate was 33 ml/min: that of CO was 0.33 ml/min, and the rest of the flowing gas was air.

CO oxidation. However, our early study [14] revealed that the presence of water vapor in the reactor enhanced the activity of the reduced Au/Y_1 even more. Therefore, all of our results support the view of Kung and co-workers [17–19] that the active gold particles for CO oxidation are nano-sized gold with hydroxyl group on its surface.

However, as shown in Fig. 6, Au/Y_2 exhibited completely different activities from those of Au/Y_1 for CO oxidation, even though the same total amount of gold as in Au/Y_1 was used in the reactor. Au/Y_2 was completely inactive, even though the catalyst was tested under the same reaction conditions for 20 h. Fig. 1 presents the results of TPR experiments, which indicated that the gold species in fresh-dried Au/Y_1 and Au/Y_2 should be similar, because similar reduction temperatures were measured. Therefore, the initial activities from these two samples should be close to each other. However, the completely different catalytic activities of Au/Y_1 and Au/Y_2 after the initiation period (4 h) during the reaction tests indicate that, the gold species in these two catalysts should be different after initiation. Table 1 reveals that the aluminum loading in Au/Y_1 (12.4%) is about seven times of that in Au/Y_2 (1.8%), and the molar ratios of gold to aluminum are about the same in both Y-type zeolites. These results suggest that the activity of gold within Y-type zeolite is strongly related to the aluminum loading in the catalyst; in other words, the density of gold or the density of aluminum on the surface of Y-type zeolite strongly influences the catalytic activity of gold for CO oxidation. However, why did the aluminum loading influence the catalytic activity of nano-gold? Aluminum in the framework of zeolite is believed to be able to prevent the sintering of gold on the surface, and the size of gold particles may strongly affect the catalytic activity; moreover, the amount of aluminum can

change the hydrophilic and the hydrophobic properties of the zeolite surface. Au/Y_2 contains much less aluminum, so the TEM and HRTEM results in the previous sections indicated that the gold particle sizes in Au/Y_2 were larger than those in Au/Y_1. Even for fresh-dried Au/Y_2, severe aggregation of gold particles was observed on the surface. The larger gold particles on Au/Y_2 were responsible for the fewer active sites and the exposure of less surface area for CO oxidation, even though the same mass of gold as in Au/Y_1 was used for the reaction. Therefore, the catalytic activity of Au/Y_2 should be lower than that of Au/Y_1.

Nevertheless, the larger gold particles on Au/Y_2 than those on Au/Y_1 do not suffice to explain the complete lack of activity of Au/Y_2 even following the 4 h initiation period (in contrast to 100% CO conversion over Au/Y_1). Other reasons must apply, one of which may be that the surface of Y_2 is more in hydrophobic than that of Y_1, because Y_2 has many fewer aluminum sites than Y_1. Therefore, much less water on the surface of Y_2, which fact may be responsible for the removal of water generated from the condensation of hydroxyl groups on the surface of gold species, which are supported on Y_2. Accordingly, the hydrophobic surface of Y_2 cannot maintain hydroxyl groups on the surface of nano-gold, even after the initiation period for Au/Y_2 and following the formation of gold metal on the surface of the zeolite. The lack of hydroxyl groups on the gold surface simply is such that catalytic activity for CO oxidation cannot be initiated.

When gold was prepared in mordenite and in β zeolite, both Au/mordenite and Au/β exhibited initial CO conversions of around 20%. However, they deactivated very rapidly in the first five hours, and declined to less than 5% CO conversion, as shown in Fig. 6. In fact, the activity of Au/β was initially slightly better than that of Au/mordenite, although the aluminum loading in β (3.2%) was only half that in mordenite (6.7%) and about twice that in Au/Y_2, as presented in Table 1. The higher loadings of aluminum in Au/β and in Au/mordenite than in Au/Y_2 may cause the lower migration and the less sintering of gold particles on the surface; moreover, the surfaces of both samples are less hydrophobic than that of Au/Y_2. This fact may explain why they both exhibited catalytic activities for CO oxidation. However, substantial decays occurred in Au/β and Au/mordenite, unlike in Au/Y_1; and the catalytic activity of Au/mordenite was much lower than that of Au/Y_1, although the gold loadings in these two zeolites were in a narrow range. These were because the channels in Au/mordenite and Au/β have smaller pore than those of the cages in Au/Y. They can be easily plugged by the gold particles. During CO oxidation, only the gold particles closed to the pore opening of the channels were easily exposed, enabling them to exhibit catalytic activity. Therefore, the resistance of the reactants toward mass transfer into the inner channels for the reaction in Au/mordenite and Au/β was responsible for the much lower catalytic activity of these two catalysts than that of Au/Y_1. Moreover, the exothermic heat of reaction during CO oxidation can provide energy for the migration and sintering of gold particles inside one-dimensional free space of the channels. This situation differs from the reactions in the cage-like Y-type zeolite. The cage can prevent the migration of gold particles, when the sizes of gold particles within the cage are larger than the cage-window (7.4 Å). Therefore, the gold particles in the channels of Au/mordenite and Au/β exhibit higher decaying rates than those in the cages of Au/Y_1.

The results presented in Fig. 6 reveal that no initiation period is required for the activation of the catalytic activity of Au/mordenite and Au/β. Notably, the first experimental data point was measured approximately 30 min after the start of the catalytic activity test for each sample. The first data points show that CO conversions from Au/mordenite and Au/β were much less than that of Au/Y_1; nevertheless, the reaction activity on Au/Y_1 continued to grow thereafter, unlike those on Au/mordenite and Au/β were decaying. This result suggests that the decays of Au/mordenite and Au/β were much faster than the activity initiation rates after 30 min or less on stream; therefore, only deactivations were observed from these two catalysts.

4. Conclusions

1. The gold loading in zeolite depended strongly on the aluminum loading in zeolite, and on the shape and the pore structure of zeolite.
2. HRTEM investigations indicated that larger gold particles were formed in Y-type zeolite with the lower aluminum loading (1.8 wt.% Al); the smaller gold particles were in Y-type zeolite with the higher aluminum loading (12.4 wt.% Al). Gold particle sized approximately 1 nm within the supercage were observed from both fresh-dried Au/Y samples.
3. The TPR study indicated that the reduction of gold species in different type zeolite by hydrogen depended on the structure of zeolite. Higher temperatures were required for the reduction in Y-type zeolite; the lower temperatures were required for β or mordenite zeolite. These results suggest that larger gold species were formed in the larger pores of Y-type zeolite; in contrast, smaller gold species were formed in the smaller pores of β or mordenite zeolite.
4. The catalytic activity for CO oxidation depended on aluminum loading, when Y-type zeolite was used for loading gold. The higher loading of aluminum on the surface of Y-type zeolite can prevent the sintering of the gold species and can provide a more hydrophilic environment for the gold species; therefore, it can provide higher catalytic activity for CO oxidation.
5. The fresh-dried gold species on Y-type zeolite prepared herein in this research is not the catalytic active species for CO oxidation. It requires an initiation period under CO oxidation reaction conditions to activate the gold species.

6. The catalytic activity and the stability of gold in Y-type zeolite (12.4 wt.% Al) were much better than those of gold in β or mordenite zeolite, because the straight channels in β or mordenite zeolite facilitated the sintering of gold. In contrast, the cage-like pores in Y-type zeolite can prevent the sintering of gold during CO oxidation.

Acknowledgements

The authors would like to thank Dr. Hong-Ping Lin (supported by CTCI Foundation in Taiwan) for taking HRTEM pictures. The financial support from National Science Council in Taiwan is appreciated.

References

[1] M. Haruta, Catal. Today 36 (1997) 153.
[2] G.C. Bond, D.T. Thompson, Catal. Rev. -Sci. Eng. 41 (1999) 319.
[3] S. Qiu, R. Ohnishi, M. Ichikawa, J. Phys. Chem. 98 (1994) 2719.
[4] T.M. Salama, T. Shido, H. Minagawa, M. Ichikawa, J. Catal. 152 (1995) 322.
[5] T.M. Salama, R. Ohnishi, M. Ichikawa, J. Chem. Soc., Faraday Trans. 92 (1996) 301.
[6] Y.-M. Kang, B.-Z. Wan, Appl. Catal. A: Gen. 128 (1995) 53.
[7] Y.-M. Kang, B.-Z. Wan, Catal. Today 26 (1995) 59.
[8] Y.-M. Kang, B.-Z. Wan, Catal. Today 35 (1997) 379.
[9] D. Guillemot, M. Polisset-Thfoin, J. Fraissard, Catal. Lett. 41 (1996) 143.
[10] V.Yu. Borovkov, V.B. Kazansky, M. Polisset-Thfoin, J. Fraissard, J. Chem. Soc., Faraday Trans. 93 (1997) 3587.
[11] J.-N. Lin, J.-H. Chen, C.-Y. Hsiao, Y.-M. Kang, B.-Z. Wan, Appl. Catal. B: Environ. 36 (2002) 19.
[12] J.-N. Lin, B.-Z. Wan, Appl. Catal. B: Environ. 41 (2003) 83.
[13] B. Bhatia, Zeolite Catalysis: Principle and Applications, CRC Press, 1990.
[14] J.-H. Chen, Redox behavior and catalytic carbon monoxide oxidation over gold/transition metal(3d) zeolite catalysts, M.S. thesis, National Taiwan University, 1996.
[15] Y.-M. Kang, B.-Z. Wan, Appl. Catal. A: Gen. 114 (1994) 35.
[16] M.A.P. Dekkers, M.J. Lippits, B.E. Nieuwenhuys, Catal. Today 54 (1999) 381.
[17] C.K. Costello, M.C. Kung, H.-S. Oh, Y. Wang, H.H. Kung, Appl. Catal. A: Gen. 232 (2002) 159.
[18] C.K. Costello, J.H. Yang, H.L. Law, Y. Wang, J.-N. Lin, L.D. Marks, M.C. Kung, H.H. Kung, Appl. Catal. A: Gen. 243 (2003) 15.
[19] H.H. Kung, M.C. Kung, C.K. Costello, J. Catal. 216 (2003) 425.
[20] Y.-M. Kang, Preparation and characterization of chromium-cobalt and gold catalysts for catalytic combustion, Ph.D. dissertation, National Taiwan University, 1994.
[21] E.D. Park, J.S. Lee, J. Catal. 186 (1999) 1.
[22] D. Cunningham, W. Vogel, M. Haruta, Catal. Lett. 63 (1999) 43.
[23] M. Date, M. Haruta, J. Catal. 201 (2001) 221.